

# A hQCD model and its phase diagram in Einstein-Maxwell-Dilaton system

---

Rong-Gen Cai<sup>a,b</sup> Song He,<sup>a,b</sup> Danning Li,<sup>c</sup>

<sup>a</sup>*State Key Laboratory of Theoretical Physics, Institute of Theoretical Physics, Chinese Academy of Science, Beijing 100190, People's Republic of China*

<sup>b</sup>*Kavli Institute for Theoretical Physics China, CAS, Beijing 100190, China*

<sup>c</sup>*Institute of High Energy Physics, Chinese Academy of Sciences, Beijing, China*

*E-mail:* [cairg@itp.ac.cn](mailto:cairg@itp.ac.cn), [hesong@itp.ac.cn](mailto:hesong@itp.ac.cn), [lidn@ihep.ac.cn](mailto:lidn@ihep.ac.cn)

ABSTRACT: By use of the potential reconstruction approach we obtain a series of asymptotically AdS (aAdS) black hole solutions in an Einstein-Maxwell-Dilaton (EMD) system. Basing on the solutions of the system, we reconstruct a semi-analytical holographic QCD (hQCD) model with a quadratic term in warped factor. We discuss some aspects of the hQCD model, in particular we calculate the free energy of two static color sources (a heavy quark-antiquark pair) which is an important order parameter to describe confinement/deconfinement phase transition. The behavior of the free energy with respect to temperature and chemical potential is studied. We find that in the hQCD model the deconfinement phase transition can be realized and a critical point occurs. The resulting phase diagram in the temperature-chemical potential  $T-\mu$  plane is in quite good agreement with the one from recent lattice results and effective models of QCD.

KEYWORDS: Einstein-Maxwell-Dilaton, black hole solution, QCD phase diagram, AdS/CFT

---

## Contents

<b>1</b>	<b>Introduction</b>	<b>1</b>
<b>2</b>	<b>Einstein-Maxwell-Dilaton system</b>	<b>4</b>
<b>3</b>	<b>Black hole solutions and associated thermodynamics</b>	<b>6</b>
<b>4</b>	<b>The hQCD model with a quadratic correction in warped factor</b>	<b>8</b>
<b>5</b>	<b>Heavy quark potential, Polyakov loop and QCD Phase diagram</b>	<b>11</b>
5.1	Heavy quark potential and Polyakov loop	11
5.2	QCD phase diagram	13
<b>6</b>	<b>Conclusion and discussion</b>	<b>19</b>
	<b>Appendices</b>	<b>19</b>
<b>A</b>	<b>Two analytical black hole solutions in EMD system</b>	<b>20</b>

---

## 1 Introduction

Understanding strongly coupling QCD related to the RHIC and LHC experiments is attracting much attention. Although a powerful method for this subject, the lattice QCD, is being developed, when it comes to the famous sign problem, lattice techniques are not well adapted to the case with finite real chemical potential  $\mu$  and no many results have been produced so far. The other effective approaches, models and effective field theories also suffer from some problems in the dense matter case. On the other hand, the gauge/gravity duality [1–4] developed in string theory, can offer new insights to hadron theory [5–12] and strongly interacting quark gluon plasma (QGP) [13–20] in top-down and bottom-up setups. The duality approach can easily deal with the dense matter problem at least for the case in the deconfinement phase. However, for the hadron phase, the current status is still not very satisfied because the builded phase diagram so far [21–24] is different from that of the real QCD [25–27]. One is expecting to build up a holographic model which can completely recover the phase diagram of the real QCD.

If one considers a system with graviton and dilaton [28–32], one can obtain solutions of Einstein equations by using the potential reconstruction method proposed in [33, 34]. However, in previous works, the back reacted geometry of the hadronic phase is not fully identified: if one wants to consider the degrees of freedom of quarks, one should take  $U(1)$  gauge field into consideration in the bulk [21, 22, 35–41]. Adding the additional field to the graviton-dilaton system, the  $U(1)$  gauge field is dual to the baryon number current

$J_D = \psi^\dagger(x)\psi(x)$ , one may generate a chemical potential by turning on an appropriate electric field in the black hole geometry. On the other hand, in QCD the effect of finite quark density is introduced by adding the term  $J_D = \mu \psi^\dagger(x)\psi(x)$  to the Lagrangian in the generating functional, so that the chemical potential  $\mu$  appears as the source of the quark density operator. According to *AdS/CFT* correspondence, the source of a QCD operator in the generating functional is the boundary value of a dual field in the bulk; therefore, the chemical potential can be considered as the boundary value of the time component of a  $U(1)$  gauge field  $A_M$  dual to the vector quark current. Note that the  $U(1)$  denotes the gauge symmetry in the bulk and global symmetry on the boundary. The symmetry is held by physical requirement of preservation of baryon number. Motivated from the holographic description of unquenched QCD system, we will design a graviton-dilaton- $U(1)$  gauge field system to accommodate the degrees of freedom in full QCD.

The confinement/deconfinement phase transition in QCD phase diagram is a very interesting issue to play with holography. In holographic QCD, it has been widely believed that the confinement phase in the pure Yang-Mills theory corresponds to the AdS  $D4$  soliton in gravity and the deconfinement phase corresponds to the black  $D4$  brane pointed out by [42]. [43] argued that deconfinement in hard wall and soft wall models occurs via a first order Hawking-Page type phase transition between a low temperature thermal AdS space and a high temperature black hole. [44] extended this discussion by studying (charged) AdS black holes with spherical or negative constant curvature horizon. The authors of [42] and [45] investigated the deconfinement phase transition by introducing hard wall in the AdS/Reissner-Nordström black-hole with using Hawking-Page phase transition. Recently, the authors of [46] and [47] carefully considered the correspondence between phases and gravity backgrounds proposed by [42] and argued that the alternative gravitational configuration named localized soliton would be properly related to the deconfinement phase. The deconfinement transition can be realized as a Gregory-Laflamme type transition. There are also various studies on Polyakov loop [48–52] to investigate QCD phase structure within hQCD models. We will propose a hQCD model and study its phase structure by studying the behavior of Polyakov loop operator in this model.

In this paper, we will extend the potential reconstruction approach [33, 34] to an Einstein-Maxwell-Dilaton (EMD) system and build up a hQCD model with a positive quadratic term in warped factor of the bulk metric. Furthermore, we will calculate the free energy of two connecting Polyakov loop operators from holographic point of view to check whether the holographic model can realize the deconfinement phase transition. We introduce the quadratic correction term in warped factor to construct the gravity configuration with asymptotic AdS UV behavior. The motivation of choosing the quadratic correction is that the quadratic correction plays important roles to realize various facts in low energy QCD. The work [53] by introducing the dilaton with form of  $e^{-c^2 z^2}$  can realize the Regge behavior of hadron spectrum which can not be achieved in hard wall hQCD model [5][54]. Andreev and Zakharov introduced a positive quadratic correction,  $e^{cz^2}$  with  $z$  the holographic coordinate and  $c > 0$ , to the warp factor of AdS<sub>5</sub> geometry. It turns out it is helpful to realize the linear behavior in heavy quark potential [55]. The linear heavy quark potential can also be obtained by introducing other deformed warp factors,

e.g. the deformed warp factor which mimics the QCD running coupling [56], and the logarithmic correction with an explicit IR cutoff  $\log \frac{z_{IR}-z}{z_{IR}}$  [57]. To produce the linear Regge behavior of the hadron excitations, Karch, Katz, Son and Stephanov [53] proposed the soft-wall AdS<sub>5</sub> model or KKSS model by introducing a quadratic correction to dilaton background in the 5D meson action, whose effect in some sense looks like introducing a negative quadratic correction,  $e^{-cz^2}$  in the warp factor of the AdS<sub>5</sub> geometry. However, it is worth mentioning that the model with a quadratic correction in the warp factor of the metric is not equivalent to the model with a quadratic correction in the dilaton background, although both models give the same effective potential of hadron spectrum in the IR region [28, 29]. A positive quadratic correction  $e^{cz^2}$  in the dilaton background of the 5D hadron action has also been used to investigate hadron spectra [58, 59], however, higher spin excitations in this background will lead to imaginary mass [12, 60] and they also are inconsistent in the gluon sector. There are the flavor models [61–63] taking into account the chiral condensation. In [64, 65], the modified five-dimensional metric at the infrared region is constructed to obtain a nontrivial dilaton solution, which incorporates the chiral symmetry breaking and linear confinement. The modified factor is leading terms  $1 + k^2 z^2$  in  $e^{k^2 z^2}$ . They do predict the mass spectra of resonance states in the pseudoscalar, scalar, vector and axial-vector mesons, which agree with experiment data. [66] also confirmed that the quadratic term in dilaton plays an important role in linear confinement in the meson sector. Recently, based on the AdS Reissner-Nordström black hole metric the work [67] introduced the  $e^{k^2 z^2}$  term in the dilaton, it turns out to be helpful to realize the heavy quark potential. All these studies mentioned above do not consider effects of back reaction of dilaton and/or a modified warped factor. The work [57] studied the topic in a non-critical string framework with back reaction effects and found that the quadratic term  $e^{k^2 z^2}$  in warped factor is helpful to achieve the Cornell potential. The work [33] further confirmed the conclusion from thermal hQCD perspective. In some sense, a positive quadratic term captures some important QCD features, although we still do not well understand. Therefore we choose the warped factor with a positive quadratic correction to build up an effective hQCD model.

The organization of the paper is as follows. In Section 2 we briefly introduce the potential reconstruction approach and apply it to an Einstein-Maxwell-Dilaton system (EMD). In Section 3, we impose asymptotical AdS boundary conditions and regularity requirements on generic black hole solutions and figure out general formulas of thermodynamic quantities of the black holes. In Sections 4, we make use of the reconstruction approach to propose our hQCD model with a positive quadratic  $k^2 z^2$  term in warped factor and calculate relevant thermodynamic quantities such as temperature, entropy, etc, of the background solution. We also simply check the stability of dilaton potential from AdS/CFT perspective. In Section 5, we investigate free energy of a heavy quark pair and vacuum expectation value (VEV) of Polyakov loop which is order parameter to describe the deconfinement phase transition. In this hQCD model, the deconfinement phase transition can be realized and a critical point appears. Section 6 is devoted to conclusions and discussions.

## 2 Einstein-Maxwell-Dilaton system

Let us begin with the following 5D Einstein-Maxwell-Dilaton (EMD) action in string frame

$$S_{5D} = \frac{1}{16\pi G_5} \int d^5x \sqrt{-g^S} e^{-2\phi} \left( R^S + 4\partial_\mu \phi \partial^\mu \phi - V_S(\phi) - \frac{1}{4g_g^2} e^{\frac{4\phi}{3}} F_{\mu\nu} F^{\mu\nu} \right), \quad (2.1)$$

where  $G_5$  and  $g_g$  are 5D Newtonian constant and effective gauge coupling constant,  $g^S$  and  $V_S(\phi)$  are the 5D metric and dilaton potential in the string frame, respectively.

To solve this system, it is convenient to transform this action to Einstein frame. If the metric in Einstein frame  $g_{\mu\nu}^E$  and its corresponding one in string frame  $g_{\mu\nu}^S$  are connected by the scaling transformation

$$g_{\mu\nu}^S = e^{\frac{4\phi}{3}} g_{\mu\nu}^E, \quad (2.2)$$

one can derive the exact relation between two actions in string frame and Einstein frame

$$\begin{aligned} & \int \sqrt{-g^S} e^{-2\phi} \left( R^S + 4\partial_\mu \phi \partial^\mu \phi - V_S(\phi) - \frac{1}{4g_g^2} e^{\frac{4\phi}{3}} F_{\mu\nu} F^{\mu\nu} \right) \\ &= \int \sqrt{-g^E} \left[ R^E - \frac{4}{3} \partial_\mu \phi \partial^\mu \phi - V_E(\phi) - \frac{1}{4g_g^2} F_{\mu\nu} F^{\mu\nu} \right] \end{aligned} \quad (2.3)$$

up to a total derivative term, where

$$V_S = V_E e^{\frac{-4\phi}{3}}. \quad (2.4)$$

Thus we have the action in Einstein frame

$$S_{5D} = \frac{1}{16\pi G_5} \int d^5x \sqrt{-g^E} \left( R - \frac{4}{3} \partial_\mu \phi \partial^\mu \phi - V_E(\phi) - \frac{1}{4g_g^2} F_{\mu\nu} F^{\mu\nu} \right), \quad (2.5)$$

where  $F_{\mu\nu} = \partial_\mu A_\nu - \partial_\nu A_\mu$  is Maxwell field. Note that here we do not consider the coupling between gauge field and dilaton field in Einstein frame.

For our aim, we are looking for black hole solutions of the system. In string frame we suppose the metric is of the form

$$ds_S^2 = \frac{L^2 e^{2A_s}}{z^2} \left( -f(z) dt^2 + \frac{dz^2}{f(z)} + dx^i dx^i \right), \quad (2.6)$$

with  $L$  the radius of AdS<sub>5</sub>. We will set  $G_5 = 1$  and  $g_g L = 1$  in Section 3, 4 and 5. In Einstein frame, the metric becomes

$$ds_E^2 = \frac{L^2 e^{2A_s - \frac{4\phi}{3}}}{z^2} \left( -f(z) dt^2 + \frac{dz^2}{f(z)} + dx^i dx^i \right). \quad (2.7)$$

In Einstein frame, the gravitational field equations read

$$E_{\mu\nu} + \frac{1}{2} g_{\mu\nu}^E \left( \frac{4}{3} \partial_\mu \phi \partial^\mu \phi + V_E(\phi) \right) - \frac{4}{3} \partial_\mu \phi \partial_\nu \phi - \frac{1}{2g_g^2} \left( F_{\mu\lambda} F_\nu^\lambda - \frac{1}{4} g_{\mu\nu}^E F_{\rho\sigma} F^{\rho\sigma} \right) = 0, \quad (2.8)$$

where  $E_{\mu\nu}$  is Einstein tensor. In the metric (2.7), the  $(t, t)$ ,  $(z, z)$  and  $(x_1, x_1)$  components of the gravitational field equations are respectively

$$b''(z) + \frac{b'(z)f'(z)}{2f(z)} + \frac{2}{9}b(z)\phi'(z)^2 + \frac{b(z)^3V_E(\phi(z))}{6f(z)} + \frac{A_t'(z)^2}{24g_g^2b(z)f(z)} = 0, \quad (2.9)$$

$$\phi'(z)^2 - \frac{9b'(z)^2}{b(z)^2} - \frac{9b'(z)f'(z)}{4b(z)f(z)} - \frac{3b(z)^2V_E(\phi(z))}{4f(z)} - \frac{3A_t'(z)^2}{16g_g^2b(z)^2f(z)} = 0, \quad (2.10)$$

$$f''(z) + \frac{6b'(z)f'(z)}{b(z)} + \frac{6f(z)b''(z)}{b(z)} + \frac{4}{3}f(z)\phi'(z)^2 + b(z)^2V_E(\phi(z)) - \frac{A_t'(z)^2}{4g_g^2b(z)^2} = 0, \quad (2.11)$$

where  $b(z) = \frac{L^2 e^{2A_E}}{z^2}$ ,  $A_E(z) = A_s(z) - \frac{2}{3}\phi(z)$  and  $A_t(z)$  is electrical potential of Maxwell field. As a consistent check, turning off  $A_t(z)$  in Eqs. (2.9) -(2.11), one can easily reproduce equations of motion about the graviton-dilaton system discussed in [33].

Note that the above three equations are not independent. In (2.9)-(2.11), there are only two independent functions, therefore one of the three equations can be used to check the consistence of solutions. From those three equations one can obtain following two equations which do not concern the dilaton potential  $V_E(\phi)$ ,

$$A_s''(z) + A_s'(z) \left( \frac{4\phi'(z)}{3} + \frac{2}{z} \right) - A_s'(z)^2 - \frac{2\phi''(z)}{3} - \frac{4\phi'(z)}{3z} = 0 \quad (2.12)$$

$$f''(z) + f'(z) \left( 3A_s'(z) - 2\phi'(z) - \frac{3}{z} \right) - \frac{z^2 e^{\frac{4\phi(z)}{3} - 2A_s(z)} A_t'(z)^2}{g_g^2 L^2} = 0. \quad (2.13)$$

Eq.(2.12) is our starting point to find exact solutions of the system. Note that Eq.(2.12) in the EMD system is the same as the one in the Einstein-dilaton system considered in [33, 34] and the last term in Eq.(2.13) is an additional contribution from electrical field.

The equation of motion of the dilaton field is given as

$$\frac{8}{3}\partial_z \left( \frac{L^3 e^{3A_s(z) - 2\phi} f(z)}{z^3} \partial_z \phi \right) - \frac{L^5 e^{5A_s(z) - \frac{10}{3}\phi}}{z^5} \partial_\phi V_E = 0. \quad (2.14)$$

And the equation of motion for the Maxwell field is

$$\frac{1}{\sqrt{-g^E}} \partial_\mu \sqrt{-g^E} F^{\mu\nu} = 0. \quad (2.15)$$

It is similar the equation given by [41]. Note that in (2.9)-(2.11) we have only considered the gravitational configurations with electric charge.

We can see from the equations of motion of the system that once given a geometric structure  $A_s(z)$ , one can derive a generic solution to the system in Einstein frame. The

generic solution takes the form

$$\phi(z) = \int_0^z \frac{e^{2A_s(x)} \left( \frac{3}{2} \int_0^x y^2 e^{-2A_s(y)} A_s'(y)^2 dy + \phi_1 \right)}{x^2} dx + \frac{3A_s(z)}{2} + \phi_0, \quad (2.16)$$

$$A_t(z) = A_{t0} + A_{t1} \left( \int_0^z y e^{\frac{2\phi(y)}{3} - A_s(y)} dy \right), \quad (2.17)$$

$$f(z) = \int_0^z x^3 e^{2\phi(x) - 3A_s(x)} \left( \frac{A_{t1}^2 \left( \int_0^x y e^{\frac{2\phi(y)}{3} - A_s(y)} dy \right)}{g_g^2 L^2} + f_1 \right) dx + f_0, \quad (2.18)$$

$$V_E(z) = \frac{e^{\frac{4\phi(z)}{3} - 2A_s(z)}}{L^2} \left( r^2 f''(z) - 4f(z) (3z^2 A_s''(z) - 2z^2 \phi''(z) + z^2 \phi'(z)^2 + 3) \right. \\ \left. - \frac{3z^4 e^{\frac{4\phi(z)}{3} - 2A_s(z)} A_t'(z)^2}{2L^2 g_g^2} \right), \quad (2.19)$$

where  $\phi_0, \phi_1, A_{t0}, A_{t1}, f_0, f_1$  are some integration constants, and will be determined by suitable UV and IR boundary conditions. Generally, one cannot give the explicit form of  $V_E(\phi)$ . But for some special cases, we can use the generating function  $A_s(z)$  to obtain some analytical solutions of the graviton-dilaton-electric field system. In appendix, we give two analytical solutions which are generated by this potential reconstruction approach.

For a consistent check, one can reproduce the general solution of graviton-dilaton system given by [33] by turning off the electrical field  $A_t(z)$ . An alternative way to check is that one can set  $A_s = 0, \phi = 0, f(z) = 1, A_t(z) = 0$  to obtain a constant dilaton potential  $V_E(z) = -\frac{12}{L^2}$  as expected.

### 3 Black hole solutions and associated thermodynamics

In this section, we will work out general formulas of some thermodynamical quantities for the semi-analytical gravity solutions of the graviton-dilaton-electrical field system by using Eq.(2.16)-(2.19) for given metric ansatz in Einstein frame (2.7). Here we are interested in a series of solutions whose UV behavior is asymptotic  $AdS_5$  (aAdS). We also impose the requirements:  $f(0) = 1$ , and  $\phi(z), f(z), A_t(z)$  are regular from  $z = 0$  to  $z_h$ . Here  $z_h$  is supposed to be the black hole horizon with  $f(z_h) = 0$ . In addition, we impose  $A_t(z_h) = 0$ , which is due to the physical requirement:  $A_\mu A^\mu = g^{tt} A_t A_t$  must be finite at the black hole horizon  $z = z_h$ .

The first is how to parameterize the Hawking temperature of the black hole solution, which is defined by  $\frac{f'(z)}{4\pi}$ . A black hole solution with a regular horizon is characterized by the existence of a surface  $z = z_h$ , where  $f(z_h) = 0$ . The Euclidean version of the solution is defined only for  $0 < z < z_h$ , in order to avoid the conical singularity, the periodicity of the Euclidean time is required as

$$\tau \rightarrow \tau + \frac{4\pi}{|f'(z_h)|}. \quad (3.1)$$

This determines the temperature of the solution as

$$T = \frac{|f'(z_h)|}{4\pi}. \quad (3.2)$$

With help of  $f(0) = 1$  and black hole horizon  $z_h$ , there  $f(z_h) = 0$ , we can fix the integration constants  $f_0$  and  $f_1$  in metric function  $f(z)$  in eq.(2.18) as follows.

$$f(z) = 1 + \frac{A_{t1}^2}{g_g^2 L^2} \frac{\int_0^z g(x) \left( \int_0^{z_h} g(r) dr \int_r^x g(y)^{\frac{1}{3}} dy \right) dx}{\int_0^{z_h} g(x) dx} - \frac{\int_0^z g(x) dx}{\int_0^{z_h} g(x) dx}, \quad (3.3)$$

where  $f(0) = 1$ ,  $f_1 = -\frac{A_{t1}^2}{g_g^2 L^2} \frac{\int_0^{z_h} dx g(x) \int_0^x g(y)^{\frac{1}{3}} dy + 1}{\int_0^{z_h} g(x) dx}$ , and the function  $g(x)$  is defined as

$$g(x) = x^3 e^{2\phi(x) - 3A_s(x)}. \quad (3.4)$$

One can easily check that  $f(z_h) = 0$  from Eq.(3.3). One should confirm that there is no other  $z_h$  satisfying  $f(z_h) = 0$  in the region  $0 < z < z_h$ . From Eq. (3.2), one can easily read out the relation between temperature and the black hole horizon from Eq.(3.3) as

$$T = \left| \frac{A_{t1}^2}{4\pi g_g^2 L^2} \frac{g(z_h) \int_0^{z_h} g(r) dr \int_r^{z_h} g^{\frac{1}{3}}(y) dy - g(z_h)}{\int_0^{z_h} g(x) dx} \right|. \quad (3.5)$$

Following the standard Bekenstein-Hawking entropy formula [68], from the geometry given in Eq.(2.7), we obtain the black hole entropy density  $s$ , which is defined by the area  $A_{area}$  of the horizon

$$s = \frac{A_{area}}{4G_5 V_3} = \frac{L^3}{4G_5} \left( \frac{e^{A_s - \frac{2}{3}\phi}}{z} \right) \Big|_{z_h}, \quad (3.6)$$

where  $V_3$  is the volume of the black hole spatial directions spanned by coordinates  $x_i$  in (2.7). Note that the entropy density is determined in terms of horizon area in Einstein frame.

In order to find out exact expressions about chemical potential and charge density, we should impose proper boundary conditions on  $A_t$ . Expanding  $A_t$  near  $z = 0$ , we have

$$A_t(z) = A_{t0} + A_{t1} e^{\frac{2\phi(y)}{3} - A(y)} \left( 1 + y \left( \frac{2\phi'(y)}{3} - A'(y) \right) \right) \Big|_{y=0} z^2 + \dots \quad (3.7)$$

Having considered the boundary condition that  $A_t(z_h) = 0$ , we can obtain from Eq.(3.7) the chemical potential  $\mu$  and the integration constant  $A_{t1}$ , which is related to the black hole charge,

$$A_{t0} = \mu \quad (3.8)$$

$$A_{t1} = \frac{\mu}{\int_0^{z_h} y e^{\frac{2\phi}{3} - A_s(y)} dy} = \frac{\mu}{\int_0^{z_h} g(y)^{\frac{1}{3}} dy}. \quad (3.9)$$

Clearly the integration constant  $A_{t1}$  can be determined by chemical potential  $\mu$  and horizon  $z_h$ . From the coefficient of the  $z^2$  term in (3.7), one can obtain the charge density of the black hole configuration.

Before ending this section, we would like to stress that the integration constants appearing in  $\phi(z)$  and  $V_E(z)$  do not occur in the solutions of electrical field  $A_t(z)$  and  $f(z)$ . As stated in [34], some integration constants will make contribution to the dilaton potential



$V_E(\phi)$ , but this does not affect application of the potential reconstruction approach to the EMD system. Based on the builded gravitational configurations, one can build up various hQCD models by choosing proper  $A_s$ . In this paper, we only focus on construction of holographic model to realize the deconfinement phase transition by investigating Polyakov loop. In addition, to be of physical interest, the builded black hole solutions should be thermodynamical and dynamical stable. Therefore it is important to check the stability of the black hole solutions generally. In the next section, we will show that the mass of scalar field in our hQCD model indeed satisfies the Breitenlohner-Freedman (BF) bound.

#### 4 The hQCD model with a quadratic correction in warped factor

From various works of constructing holographic QCD models for describing the heavy quark potential and the light hadron spectra, we learn that a quadratic background correction is related to the confinement property, i.e. the linear quark anti-quark potential [57] and the linear Regge behavior[12]. A positive quadratic correction,  $e^{cz^2}$  with  $c > 0$ , in the deformed warp factor of AdS<sub>5</sub> can help to realize the linear heavy quark potential [55]. A quadratic dilaton background in the 5D meson action, whose effect in some sense looks like introducing a negative quadratic correction,  $e^{-cz^2}$ , in the warp factor of the AdS<sub>5</sub> geometry, is helpful to realize the linear Regge behavior of hadron excitations [53]. In our previous study in [33], it shows that the hQCD model with a positive quadratic correction in warped factor is favored. Therefore, we introduce the following hQCD model with a positive quadratic correction in the warp factor of AdS<sub>5</sub> in Eq.(2.6), i.e. we take

$$A_s(z) = k^2 z^2 \quad (4.1)$$

where  $k$  is a parameter related to energy scale of the model, which will be fixed later.  $A_s(z)$  is the generating function of the solution (2.16)-(2.19). In terms of the general expressions for the solution of graviton-dilaton-electric field system, we can obtain the configuration of  $\phi$  field as

$$\phi(z) = \frac{3}{4}k^2 z^2(1 + H(z)), \quad (4.2)$$

where we have set  $\phi_0 = 0$  to keep the metrics (2.6) and (2.7) are asymptotical AdS, and  $H(z)$  is

$$H(z) = {}_2F_2\left(1, 1; 2, \frac{5}{2}; 2k^2 z^2\right). \quad (4.3)$$

With  $A_s$  and  $\phi$ , we can obtain the metric function  $f$  as

$$\begin{aligned} f(z) &\equiv f(z, z_h, \mu) \\ &= 1 + \frac{1}{g_g^2 L^2} \left( \frac{\mu}{\int_0^{z_h} g(y)^{\frac{1}{3}} dy} \right)^2 \frac{\int_0^z g(x) \left( \int_0^{z_h} g(r) dr \int_r^x g(y)^{\frac{1}{3}} dy \right) dx}{\int_0^{z_h} g(x) dx} \\ &\quad - \frac{\int_0^z g(x) dx}{\int_0^{z_h} g(x) dx}, \end{aligned} \quad (4.4)$$

where

$$g(x) = x^3 e^{\frac{3}{2}k^2 x^2(1+H(x))-3k^2 x^2}. \quad (4.5)$$

With the solutions of  $A_s(z)$  and  $\phi(z)$ , one can obtain the expression of the electric field

$$A_t(z) = \mu + \frac{\mu}{\int_0^{z_h} g(y)^{\frac{1}{3}} dy} \int_0^z x e^{\frac{1}{2}k^2 x^2(-1+H(x))} dx. \quad (4.6)$$

Further one can obtain the potential of the dilaton field. The potential includes the contribution from the electrical field. The form of the potential is too complicated and therefore we do not present it here. Instead we will discuss the UV behavior of the dilaton potential to check whether the potential satisfies the constraint from the 5D Breitenlohner-Freedman (BF) bound.

The conformal invariance in the UV can be restored when  $\phi \sim 0$  at the UV boundary  $z \rightarrow 0$ . One can expand  $\phi(z)$  at UV boundary  $z \sim 0$  as

$$\phi(z \rightarrow 0) \sim \frac{3k^2 z^2}{2} + \frac{3k^4 z^4}{10} + \dots. \quad (4.7)$$

The behavior shown in Eq.(4.7) is consistent with the requirement of the asymptotic AdS<sub>5</sub> near the ultraviolet boundary.

Through the AdS/CFT dictionary, for any scalar field  $\Phi$ , we have

$$\lim_{\Phi \rightarrow 0} V(\Phi) = -\frac{12}{L^2} + \frac{1}{2L^2} \Delta(\Delta - 4)\Phi^2 + O(\Phi^4). \quad (4.8)$$

By using the following relationship

$$\partial_{\Phi}^2 V(\Phi) = \frac{\partial r}{\partial \Phi} \frac{\partial}{\partial r} \left( \frac{\partial r}{\partial \Phi} \frac{\partial V(z)}{\partial r} \right) = M_{\Phi}^2 + O(\Phi) + \dots, \quad (4.9)$$

one can easily get the conformal dimension of the scalar field. In Eq. (4.8),  $\Delta$  is defined as  $\Delta(\Delta - 4) = M_{\Phi}^2 L^2$ , which is constrained by the BF bound  $2 < \Delta < 4$ . Comparing our case to the standard formula, one should notice the reation  $\Phi = \sqrt{\frac{8}{3}}\phi$ , thus we have

$$M_{\Phi}^2 = -\frac{4}{L^2}. \quad (4.10)$$

Therefore, the conformal dimension of the dilaton field is  $\Delta = 2$  in our model. The dilaton therefore satisfies the BF bound but does not correspond to any local, gauge invariant operator in 4D QCD. Although there have been some discussions in recent years of the possible relevance of a dimension two condensate in the form of a gluon mass term [69], it is not clear whether we can associate  $\phi$  with dimension-2 gluon condensate, because the AdS/CFT correspondence requires that bulk fields should be dual to gauge-invariant local operators. This situation is the same as the case in the recent paper [33]. Note that in the potential reconstruction approach, the electrical field does not change the configuration of dilaton and the UV behavior of the dilaton potential.

Once the metric function  $f$  is given, one can easily find the relation between the black hole temperature and the horizon radius  $z_h$ . In figure 1 we plot the relation between the temperature and horizon with different chemical potential. One can see from figure 1 that the black hole temperature can not reach zero temperature if the chemical potential is zero. On the other hand, if one turns on a nonvanishing chemical potential, the lowest temperature can reach zero, this case corresponds to an extremal black hole. In the case with a nonvanishing chemical potential, as one can see from the figure that the behavior of the temperature heavily depends on the value of chemical potential. Basically the behavior of the temperature can be classified into two cases: when chemical potential  $\mu > \mu_c$ , the temperature decreases monotonically to zero as  $z_h$  increases, while if  $\mu < \mu_c$ , it decreases monotonically to a minimum at  $z_m$ , then goes to a maximum at  $z_M$  and then decreases to zero. The critical chemical potential depends on the parameter  $k$ . In our model, we take parameter  $k = 0.3\text{GeV}$ , which is consistent with the lattice data for equation of state, heavy quark potential and so on [33]. We have checked that if one changes the value of  $k$ , our conclusions in this paper do not change qualitatively. In the case of  $k = 0.3\text{GeV}$ , the corresponding critical chemical potential  $\mu_c = 0.34\text{GeV}$ . Here the critical chemical potential is determined by  $T(\mu = \mu_c, z_h = z_m) = T(\mu = \mu_c, z_h = z_M)$ . And  $z_m$  and  $z_M$  have been presented in figure 2.

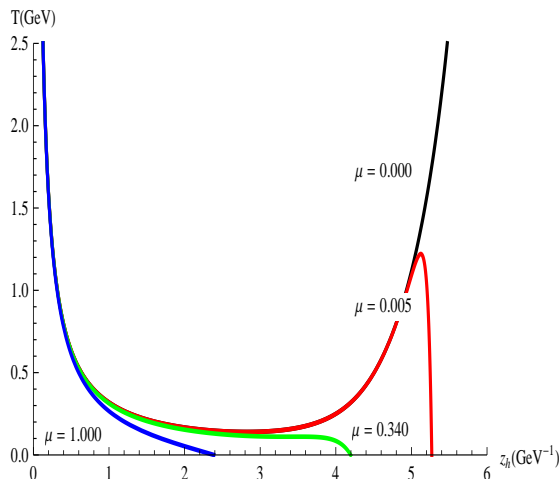


**Figure 1.** The black hole temperature versus horizon  $z_h$  with different chemical potential. When  $\mu = 0$ , the temperature behavior is similar to the case considered in [33]. When  $\mu > \mu_c$  the temperature monotonically decreases to zero as  $z_h$  increases. While  $0 < \mu < \mu_c$ , the temperature decreases to a minimum at  $z_m$  and then grows up to a maximum at  $z_M$  and then decreases to zero monotonically. When  $\mu = \mu_c$ , one has  $z_m = z_M$ .  $z_m$  and  $z_M$  are marked explicitly in figure 2. In our model, we fix  $k = 0.3\text{GeV}$  and accordingly the critical chemical potential is  $\mu_c = 0.34\text{GeV}$ .

From the behavior of the temperature, one can see that the black hole solution is locally thermodynamical stable when  $\mu > \mu_c$ , because in this case, the heat capacity of the solution is positive (Note that the horizon size of the black hole is  $1/z_h$ ). On the other hand, the case with  $\mu < \mu_c$  has to be discussed separately. To clearly see the stability of the black

hole solution in the case  $\mu < \mu_c$ , in figure 2 we plot the temperature versus the horizon  $z_h$  in the case  $\mu = 0.1\text{GeV} < \mu_c$ . We can see from the figure that the background black hole is thermodynamical unstable in the region  $z_m < z_h < z_M$ , where  $z_m$  and  $z_M$  are the black hole horizons, respectively, corresponding to the minimal and maximal temperatures. In this region, the heat capacity of the black hole is negative. The black hole solutions in the regions  $z_h < z_m$  and  $z_h > z_M$  are thermodynamical stable. When  $\mu = \mu_c$ ,  $z_m$  and  $z_M$  are degenerated to one point.

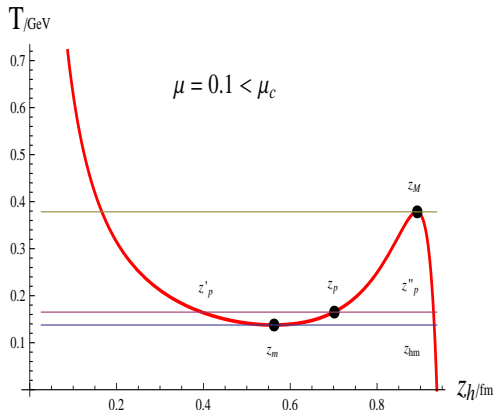


**Figure 2.** The temperature of the black hole with  $\mu = 0.1\text{GeV}$ . The three black hole solutions with horizon  $z'_p$ ,  $z_p$  and  $z''_p$  have the same temperature. The black hole with  $z_m < z_p < z_M$  is thermodynamically unstable. In the figure we take  $g_f L = 1, k = 0.3\text{GeV}$ .

The existence of the critical chemical potential plays a crucial role to realize the critical point in QCD phase diagram. We will see this in the next section by calculating the heavy quark potential in this hQCD model.

## 5 Heavy quark potential, Polyakov loop and QCD Phase diagram

To investigate some properties of the hQCD model constructed in the previous section, let us study an infinitely heavy quark-antiquark pair, at distance  $r$  from each other. It is interesting to investigate how the free energy of such a system changes with temperature and chemical potential by using the holographic description of loop operators [70–72]. The free energy is a proper quantity to describe the confinement/deconfinement phase transition.

### 5.1 Heavy quark potential and Polyakov loop

At finite temperature, the free energy  $F(r, T)$  of an infinitely heavy quark-antiquark pair at distance  $r$  can be obtained in QCD from the correlation function of two Polyakov loops [72]

$$\langle \mathcal{P}(\vec{x}_1) \mathcal{P}^\dagger(\vec{x}_2) \rangle = e^{-\frac{1}{T} F(r, T) + \gamma(T)} \quad (5.1)$$

with  $r = |\vec{x}_1 - \vec{x}_2|$  and  $\gamma(T)$  a normalization constant. Moreover, the vacuum expectation value of a single Polyakov loop

$$\langle \mathcal{P} \rangle = e^{-\frac{1}{2T} F^\infty(T)} \quad (5.2)$$

( $F^\infty(T) = F(r = \infty, T)$  and the normalization factor is neglected) is an order parameter for the deconfinement transition of a gauge theory [72]. Within the gauge/string duality approach, we can attempt a calculation of the expectation values in (5.1) and (5.2) by considering a fundamental string configuration with Polyakov loop on the boundary. The Nambu-Goto action of the string is

$$S_{\text{NG}} = \frac{1}{2\pi\alpha'} \int d^2\xi \sqrt{\det[g_{ab}]} = \frac{1}{2\pi\alpha'} \int d^2\xi \sqrt{\det[g_{MN} (\partial_a X^M) (\partial_b X^N)]} \quad (5.3)$$

In terms of the geometry background  $g_{MN}$  given by (2.6), the induced metric  $g_{ab}$  can be expressed as

$$g_{ab} = \begin{pmatrix} -\frac{e^{2A_s(z)} f(z)}{z^2} & 0 \\ 0 & \frac{e^{2A_s(z)} \left( \frac{1}{f(z)} \frac{dz^2}{dx^2} + 1 \right)}{z^2} \end{pmatrix}, \quad (5.4)$$

where we have chosen the static gauge  $\xi^0 = t$  and  $\xi^1 = x$ . We are interested in the configurations of two static quarks on the boundary. The configurations should obey the boundary conditions:  $z(x=0) = z_0$  and  $z'(x=0) = 0$  and  $z(x = \pm \frac{r}{2}) = 0$ . Here the prime stands for the derivative with respect to  $x$ . There are two independent configurations as shown in figure 3 which satisfy the boundary conditions. Figure 3(a) stands for the case with two static quarks linked by a fundamental string. This configuration describes the confining phase. Figure 3(b) describes the case where the string is broken into two segments, each of them extends to the horizon of black hole. This configuration stands for two static decoupled quarks, which corresponds to the deconfinement phase. The configuration in figure (a) corresponds to the ‘‘Minkowski embedding’’, while figure (b) to the ‘‘black hole embedding’’ in the  $D_3/D_7$  setup [73].

From (5.3) and (5.4), we obtain the free energy of the string configuration

$$F(r, T) = \frac{g_p}{\pi} \int_{-r/2}^0 dx \frac{e^{k^2 z^2}}{z^2} \sqrt{f(z) + (z')^2}, \quad (5.5)$$

where  $g_p = \frac{L^2}{\alpha'}$ . One can see from (5.5) that the configuration of the string satisfies the constraint

$$H = \frac{e^{k^2 z^2}}{z^2} \frac{f(z)}{\sqrt{f(z) + (z')^2}}, \quad (5.6)$$

where  $H$  is a conservation quantity, the Hamiltonian of the string configuration.

For later convenience, we express  $F(r, T)$  in terms of  $z_0$  and  $f_0 = f(z)|_{z=z_0}$ . Defining  $v = \frac{z}{z_0}$ , and subtracting the UV ( $v \rightarrow 0$ ) divergence in (5.5), which corresponds to subtract the infinite quark and antiquark mass in four dimensional QCD [70], we obtain the regularized free energy for the string configuration in the confining phase

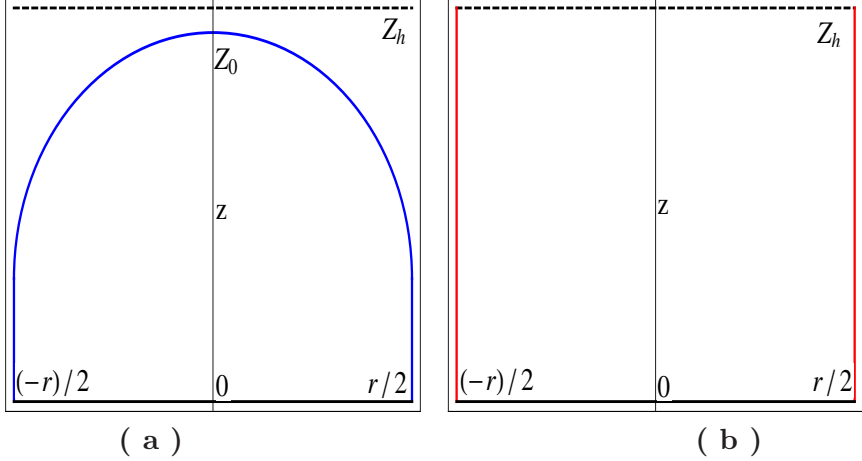


**Figure 3.** The two configurations represent the confinement phase and deconfinement phase. In Figure (a) there is a fundamental string connecting with two static quarks on the boundary. This configuration denotes the confining phase. In Figure (b) one string beaks into two segments, both of them extend to the horizon of the black hole. This configuration corresponds to the deconfinement phase.

$$\hat{F}(\lambda, T) = \frac{g_p}{\pi\lambda} \left[ -1 + \int_0^1 \frac{dv}{v^2} \left( \frac{e^{\lambda^2 v^2}}{\tau(v)} - 1 \right) \right], \quad (5.7)$$

where  $\hat{F} = F/k$ ,  $\lambda = k z_0$  and

$$\tau(v) = \sqrt{1 - \frac{f_0}{f(z_0 v)} v^4 e^{2\lambda^2(1-v^2)}}. \quad (5.8)$$

The distance  $\hat{r} = kr$  can also be parameterized by  $z_0$ ,

$$\hat{r}(z_0) = 2\lambda^2 \sqrt{f_0} \int_0^1 dv \frac{v^2 e^{\lambda^2(1-v^2)}}{\tau(v) f(z_0 v)}. \quad (5.9)$$

Next we calculate the regularized free energy for the configuration in the deconfinement phase. In this case, one has  $z_0 = z_h$ . Using the gauge  $\xi^0 = t$  and  $\xi^1 = z$  and  $x'(z) = 0$ , we obtain the regularized free energy

$$\hat{F}^\infty(\hat{T}) = \frac{g_p}{\pi} \left[ -\frac{1}{\hat{z}_h} + \int_0^{\hat{z}_h} \frac{d\hat{z}}{\hat{z}^2} \left( e^{\hat{z}^2} - 1 \right) \right] + \zeta(\hat{\mu}, \hat{T}), \quad (5.10)$$

where  $\hat{T} = T/k$  and  $\hat{z} = kz$ .  $\zeta(\hat{\mu}, \hat{T})$  is a term related to the regularization procedure, and we identify the maximum of the free energy  $\hat{F}(r, T)$  with  $\hat{F}^\infty$  to fix the regularization term following [67].

## 5.2 QCD phase diagram

In this subsection, we will discuss the phase diagram of the hQCD model by analyzing the regularized free energies obtained in the previous subsection for those two different configurations.

To analyze the behavior of  $\hat{r}(z_0)$  is helpful to distinguish two different phases. Note that there might exist a divergence in (5.9) for some parameters due to a vanishing  $\tau(v)$ . An infinite  $\hat{r}$  in figure 2(a) implies that two static quark are still coupled even with infinite separation. This means that the case with the infinite  $\hat{r}$  is in the confining phase. If there does not exist any divergence in  $\hat{r}(z_0)$ , one can find a maximum  $\hat{r}_{\max}$  at some  $z_0$  with fixed chemical potential  $\mu$  and temperature  $T$ . Beyond  $\hat{r}_{\max}$ , the string configuration in the confining phase becomes unstable, and the deconfinement phase transition happens in this case.

We can see from (5.8) that when  $v = 1$ , one has  $\tau = 0$ . This means that the divergence in (5.9) appears when  $\tau = 0$ . Note that other factors in (5.9) do not lead to any divergence. Let us first analyze the behavior of  $\tau(v)$  near  $v = 1$ . Expanding the quantity in the square root in  $\tau(v)$  at  $v = 1$ , one has

$$\tau(v) \sim \sqrt{c_1(1-v) + c_2(1-v)^2 + \mathcal{O}((1-v)^2)}, \quad (5.11)$$

where  $c_1$  and  $c_2$  are two expansion coefficients. Note that the following relations

$$\begin{aligned} \int_0^1 dv \frac{1}{\sqrt{1-v}} &= 2, \\ \int_0^1 dv \frac{1}{1-v} &= \infty. \end{aligned} \quad (5.12)$$

We can see that if  $c_1 = 0$ , the integration in (5.9) is divergent, otherwise it always gives a finite result. Furthermore we find that  $c_1$  is of the following form

$$c_1 \sim \frac{z_0}{f(z_0, z_h, \mu)} \frac{df(z_0, z_h, \mu)}{dz_0} + 8k^2 z_0^2 - 4, \quad (5.13)$$

with positive  $z_h, \mu$  and  $0 < z_0 < z_h$ . Note that the first term in the right hand side in (5.13) is negative due to  $\frac{\partial f(z, z_h, \mu)}{\partial z} < 0$  in the region  $z_0 < z_h$ , and the second term is always positive. Therefore, in the case with fixed  $\mu$ , if  $z_h$  is large enough,  $c_1$  can reach zero at some  $z_0 (< z_h)$ . At that point,  $\hat{r}(z_0)$  is divergent. On the other hand, in some region of parameters  $z_h$  and  $\mu$ ,  $c_1$  is always positive definite and  $\hat{r}(z_0)$  is then finite in that region. Let us stress again that the case with a vanishing  $c_1$  is always in the confining phase, while the case with positive definite  $c_1$  corresponds to deconfinement phase. In figure 4 we show the behavior of  $c_1$  with respect to  $z_0$  for various  $z_h$  and a fixed chemical potential  $\mu = 0.1\text{GeV}$ .

One can also obtain free energy  $F$  of the static quark-antiquark potential in two different phases through (5.7). In figure 5, we plot the function  $r(z_0)$  with a fixed  $\mu = 0.1\text{GeV}$ . We see clearly that when  $z_h < z_p$  and then  $c_1 > 0$ ,  $r(z_0)$  has a maximum  $r_{\max}$ . This case corresponds to the deconfinement phase. On the other hand, the  $z_h \geq z_p$  cases correspond to the confining configuration in which there exists a divergence in the blue curve  $r(z_0)$ . In the confining phase, if the separation  $r(z_0)$  of two static quarks can go to infinity, the phase is called permanent confinement phase. The red and pink solid curves correspond to the deconfinement case. In these cases, there exist some maximums in the curves  $r(z_0)$

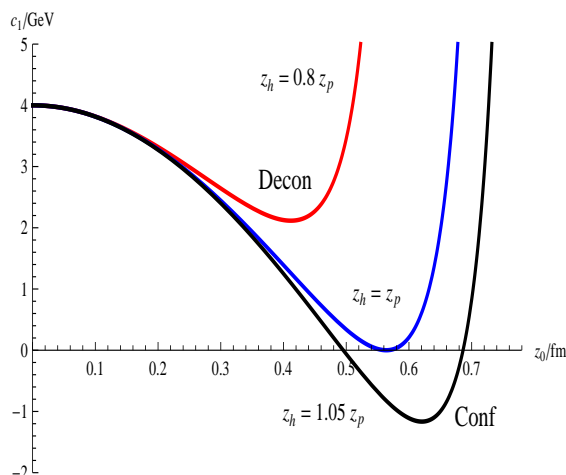


**Figure 4.** This plot shows the behavior of  $c_1$  with respect to  $z_0$  with three different black hole horizons  $z_h$  and a fixed chemical potential  $\mu = 0.1\text{GeV}$ . The solid red curve represents the deconfinement phase, the solid black curve corresponds to the confinement phase, and the solid blue one denotes the deconfinement phase transition.  $z_p$  is the critical horizon which leads  $c_1$  to have a single zero root.  $z_h < z_p$  and  $z_h \geq z_p$  correspond to the deconfinement phase and confinement phase respectively. Here we take  $g_g L = 1$  and  $k = 0.3\text{GeV}$ .

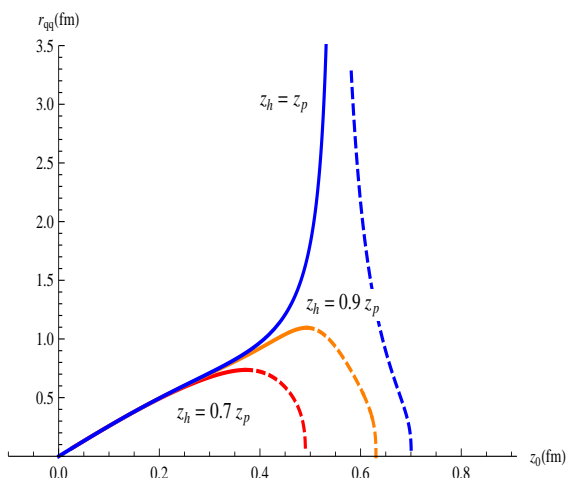


**Figure 5.** This plot shows the relation between the distance between two quarks and  $z_0$  with a fixed  $\mu = 0.1\text{GeV}$ . The blue curve corresponds to the configuration given in figure 3 (a) which stands for confining phase, while the red and pink curves correspond to the configurations given figure 3 (b). When  $z_h = z_p$ ,  $r(z_0)$  can be infinity at some  $z_0$  in  $0 < z_0 < z_h$ . The dashed curves are related to configurations in unstable region.

in  $0 < z_0 < z_h$ , beyond those maximums there are no stable configurations of two coupled quarks.

In figure 6, we plot the free energy with respect to  $z_0$  with a fixed  $\mu = 0.1\text{GeV}$ . We



can see from the figure that in the deconfinement case, the free energy has a maximum in  $0 < z_0 < z_h$ . We identify the maximum of  $F(r, T)$  with  $F^\infty(T)$  following the strategy given in [67]. In figure 7 the free energy is plotted with respect to the distance between two quarks. We see from the figure that the potential with  $z_h = z_p$  can go to infinity when  $r \rightarrow \infty$ . This means the vacuum expectation value (VEV) of polyakov loop (5.2) in this phase is vanishing, which implies the configuration is in the confining phase. On the other hand, the free energy  $F$  in the cases  $z_h = 0.7z_p$  and  $z_h = 0.9z_p$  is finite when  $r \rightarrow \infty$ . This implies that in this case the VEV of Polyakov loop (5.2) is not vanishing and the configuration is in the deconfinement phase.

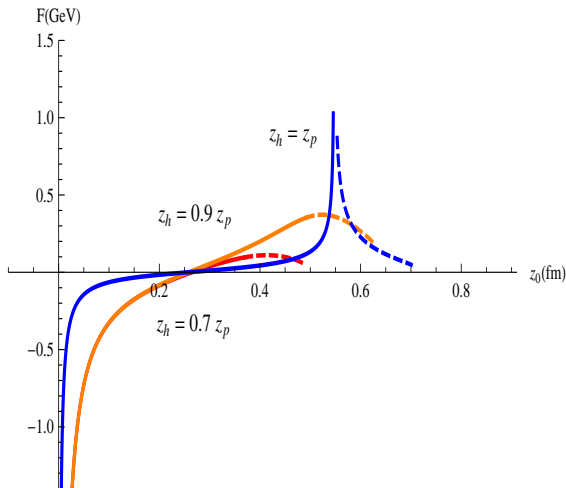


**Figure 6.** The free energy  $F$  of string configurations versus  $z_0$  with a fixed  $\mu = 0.1\text{GeV}$ . The solid blue curve corresponds to the confinement phase and the other two to the deconfinement phase. Here  $g_g L = 1, g_p = 1, k = 0.3\text{GeV}$ . The dashed curves are related to configurations in unstable region.

Through the above analysis, we see that the key point of finding phase transition in the hQCD model is to find the critical horizon  $z_h = z_p$ , for which  $\hat{r}(z_0)$  is divergent. The strategy is the same as the one employed in works [67, 74]. The numerical results in figure 5 show that one can fix the critical horizon  $z_p$  and then the phase transition temperature with a fixed chemical potential  $\mu$  through (5.13).

Let us first discuss the case with  $\mu < \mu_c$ . In this case the phase transition is a first order one. To confirm this, let us see the phase transition from the Polyakov loop perspective [75]. From our numerical study, one can see that the critical horizon  $z_p$  determined by free energy of heavy quark pair always lives in  $z_m < z_p < z_M$  when  $\mu < \mu_c$ . The phase transition temperature corresponds to the black hole having the horizon  $z_p$ . But the black hole with  $z_p$  is thermodynamical unstable. Furthermore one can see from figure 2 that there exist another two black hole solutions with horizon  $z'_p$  and  $z''_p$ , which have the same temperature as the black hole with horizon  $z_p$ . The two black hole solutions with  $z'_p$  and  $z''_p$  are thermodynamical stable. They correspond to two different phases, deconfinement phase and confinement phase, respectively. The deconfinement phase transition happens

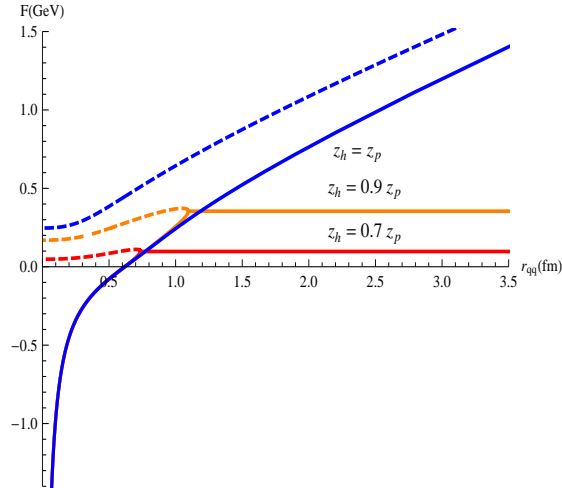


**Figure 7.** This plot show the free energy  $F(r, T)$  versus the distance  $r$  between two quarks with a fixed  $\mu = 0.1$ . The solid blue curve corresponds to the confinement phase and the other two to the deconfinement phase. In the confining phase the free energy  $F$  goes to infinity when  $r \rightarrow \infty$ . In the deconfining phase there is a maximum in  $0 < z_0 < z_h$ . Here  $g_g L = 1, g_p = 1, k = 0.3 \text{ GeV}$ . The dashed curves are related to configurations in unstable region.

from the black hole with  $z_p''$  to the one with  $z_p'$  at the transition temperature.

After fixing the phase transition temperature, next we calculate the VEV of a single Polyakov loop by using (5.10), which is a function of temperature. We find that when  $z_h > z_p$ ,  $\langle \mathcal{P} \rangle$  is always vanishing, while  $\langle \mathcal{P} \rangle$  does not as  $z_h < z_p$ . Therefore there must be a jump of  $\langle \mathcal{P} \rangle$  from 0 to a nonvanishing one in  $\langle \mathcal{P} \rangle - T$  plane as shown in figure 8(a). The black dot and red dot in the figure represent the black hole solutions with  $z_p''$  and  $z_p'$ , respectively. We can clearly see from the figure that the phase transition is a first order one in this case.

Now we discuss the case with  $\mu \geq \mu_c$ . In this case, the temperature is a monotonic function of horizon  $z_h$  as shown in figure 1. After fixing the phase transition temperature through (5.13), we calculate the VEV of the a single Polyakov loop by using (5.10). We find that when  $z_h > z_p$ ,  $\langle \mathcal{P} \rangle = 0$ , which corresponds in the confining phase, while  $\langle \mathcal{P} \rangle$  increases monotonically from 0 as  $z_h \leq z_p$ . The behavior of  $\langle \mathcal{P} \rangle$  is shown in 8(b). This case can be interpreted as a continuous transition [76]. The continuity of  $\langle \mathcal{P} \rangle$  at the phase transition point implies that the deconfinement transition might be a crossover in the heavy quark limit [77].

Combing the above analysis, we plot a naive  $T - \mu$  phase diagram in figure 9 for our hQCD model. In the figure the black dot denotes the critical point with  $\mu = \mu_c$ . When  $\mu < \mu_c$ , the deconfinement transition is a first order one, while it is a continuous transition as  $\mu > \mu_c$ . This phase diagram agrees with the expectation from effective field theory [78, 79] and recent lattice QCD simulation [76]. By using effective theory, the recent lattice QCD simulation [76] studies the deconfinement transition of QCD with heavy quark. It is found that the deconfinement transition is first order in small chemical

potential region, while it is an analytic crossover in large  $\mu$  region. Our results therefore are consistent with the lattice simulation [76]. Furthermore, note that the work [67] considered a hQCD model by introducing a warped factor to deform the AdS Reissner-Nordström black hole background and concluded that the deconfinement phase transition is a continuous phase transition. Differing from the work [67], we have constructed a self-consistent gravitational configuration by considering the back reaction of dilaton field and a critical point has been found in the phase diagram.

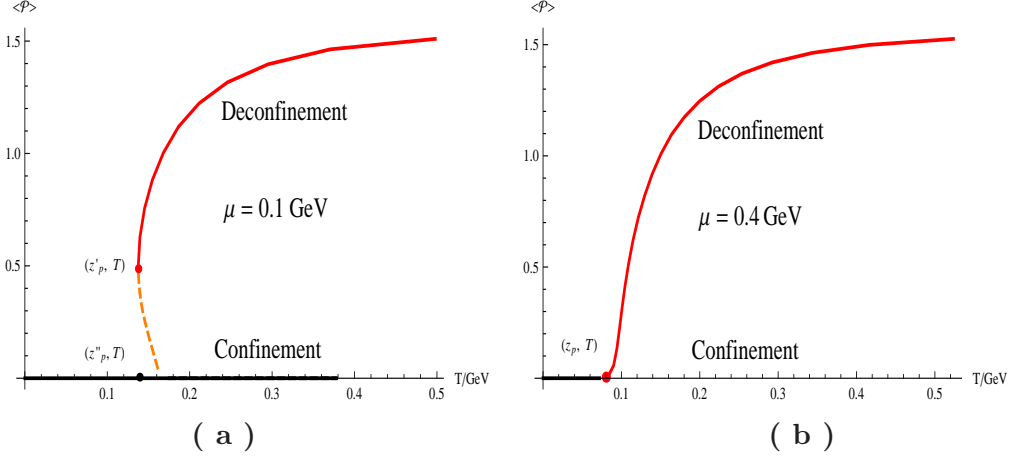


**Figure 8.** The vacuum expectation of a single Polyakov loop versus temperature. The left panel shows the case with  $\mu < \mu_c$  and the right one with  $\mu > \mu_c$ . In (a) the dashed pink curve shows the behavior of  $\langle \mathcal{P} \rangle$  in the unstable region  $z_m < z_h < z_M$ . Here  $g_p = 1, k = 0.3\text{GeV}$ .

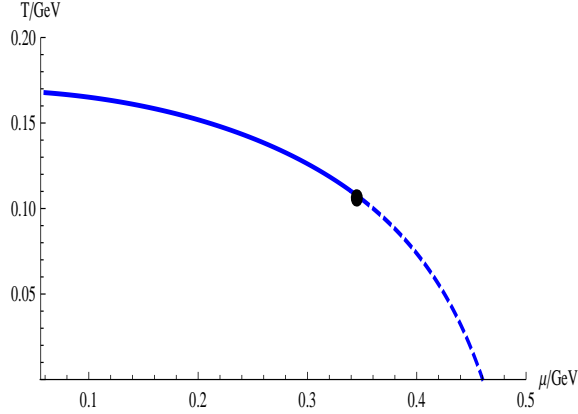


**Figure 9.** The phase diagram of the hQCD model constructed in this paper. The dashed blue curve stands for the continuous phase transition and the solid blue one for the first order phase transition. The black dot represents the critical point. Here  $g_p = 1, k = 0.3\text{GeV}$ .

## 6 Conclusion and discussion

The gravity/gauge theory duality is a powerful tool to investigate strongly coupling systems. In this spirit, one of dreams is to build a holographic description dual to a real low energy QCD theory. In this paper, by using the potential reconstruction approach [33, 34], we have given a generic formulism to find a series of asymptotically AdS black hole solutions for the Einstein-Maxwell-dilaton system. In this approach, the back reaction of dilaton and Maxwell field is taken into account. In this sense, our approach avoids some shortcomings in the literature in constructing holographic QCD models.

Based on the approach, we have constructed a self-consistent gravitational configuration to describe some properties of low energy QCD theory. The gravitational configuration includes a quadratic term in warped factor of bulk metric. The behavior of temperature of the black hole configuration is similar to that of an AdS Reissner-Nordström black hole. The quadratic term in warped factor plays an important role in the hQCD model. By calculating heavy quark potential and Polyakov loop in this hQCD model, we have analyzed the phase structure of the model. It has been found that there exists a critical point in  $T - \mu$  phase diagram. When the chemical potential  $\mu < \mu_c$ , the deconfinement phase transition is a first order one, while it is a continuous transition when  $\mu > \mu_c$ . This phase diagram is agreement with results from effective field theory [78, 79] and recent lattice QCD simulation [76]. In our model, the value of the critical chemical potential depends on the model parameter  $k$ . In our discussions,  $k = 0.3\text{GeV}$  and then  $\mu_c = 0.34\text{GeV}$ . We have checked other values of  $k$  and our results do not change qualitatively and the conclusions still holds.

In this work we have only studied the deconfinement transition of the hQCD model in heavy quark limit, by studying Polyakov loop in the black hole background presented in this paper. It would be of great interest to further investigate other aspects of the hQCD model. For example, it is required in the model to further study the spectra of hadrons, chiral phase transition [38–40], hydrodynamical properties of QGP, and color flavor locked phase [80–82], etc.. In addition, it would be also interesting to construct thermal gas solution in the EMD system and to discuss the Hawking-Page phase transition between the black hole solution and the thermal gas solution.

**Acknowledgments:** The authors thank T. Hatsuda, Mei Huang, Hong Mao, Defu Hou, Tamal Mukherjee, Dawei Pang, Fukun Xu, Jun Tao, Shunjin Wang, Junbao Wu, Haitang Yang, Qishu Yan and Yi Yang for valuable discussions. The authors specially thank Elias Kiritsis for his helpful comments and suggestions, which help us to improve this paper. S.H. appreciates the hospitality of institute of high energy physics, CAS and Physics Department of Sichuan University at various stages of this work. This work is supported in part by grants from NSFC (No. 10821504, No. 10975168 and No. 11035008). This work is also supported partially by FRFCU, No. 2011RC22.

## APPENDIX

### A Two analytical black hole solutions in EMD system

In this appendix, we give two analytical black hole solutions of EMD system by using Eqs.(2.16)-(2.19). Here we are interested in the solutions whose UV behavior is asymptotic  $AdS_5$ . We impose the constraint  $f(0) = 1$  at  $z = 0$ , and require  $\phi(z)$  and  $f(z)$  to be regular in the region  $z \in [0, z_h]$ , where  $z = 0$  is the AdS boundary and  $z_h$  corresponds to the horizon of black hole solution.

We give black hole solutions in Einstein frame. The metric in Einstein frame takes the following form

$$ds_E^2 = \frac{L^2 e^{2A_s - \frac{4\phi}{3}}}{z^2} \left( -f(z) dt^2 + \frac{dz^2}{f(z)} + dx^i dx^i \right) \quad (\text{A.1})$$

$$= \frac{L^2 e^{2A_E}}{z^2} \left( -f(z) dt^2 + \frac{dz^2}{f(z)} + dx^i dx^i \right), \quad (\text{A.2})$$

where  $A_E(z) = A_s(z) - \frac{2\phi(z)}{3}$ .

The first set of exact solutions is

$$\begin{aligned} A_E(z) &= \log \left( \frac{z}{z_0 \sinh(\frac{z}{z_0})} \right), \\ f(z) &= 1 - \frac{4V_{11}}{3} \left( 3 \sinh\left(\frac{z}{z_0}\right)^4 + 2 \sinh\left(\frac{z}{z_0}\right)^6 \right) + \frac{1}{8} V_{12}^2 \sinh\left(\frac{z}{z_0}\right)^4, \\ \phi(z) &= \frac{3z}{2z_0}, \\ A_t(z) &= \mu - \frac{2g_g L}{z_0} V_{12} \sinh\left(\frac{z}{2z_0}\right)^2, \end{aligned} \quad (\text{A.3})$$

where  $z_0$  and  $\mu$  are two integration constants,  $V_{11}$  and  $V_{12}$  are two constants from the dilaton potential, and  $g_g$  is gauge coupling. The dilaton potential is given by

$$V_E(\phi) = -\frac{12 + 9 \sinh^2\left(\frac{2\phi}{3}\right) + 16V_{11} \sinh^6\left(\frac{\phi}{3}\right)}{L^2} + \frac{V_{12}^2 \sinh^6\left(\frac{2\phi}{3}\right)}{8L^2}. \quad (\text{A.4})$$

If turn off the gauge field, one can reproduce one solution of the graviton-dilaton system given in [33][34]. On the other hand, if set  $V_{11} = 0$  and  $V_{12} = 0$ , one can reach the 5D BPS solution in [34].

The second set of exact solutions is

$$A_E(z) = -\log\left(1 + \frac{z}{z_0}\right), \quad (\text{A.5})$$

$$f(z) = 1 - V_{21} \left( \frac{z^7}{7z_0^7} + \frac{z^6}{2z_0^6} + \frac{3z^5}{5z_0^5} + \frac{z^4}{4z_0^4} \right) + \frac{\rho^2 z_0^8}{g_g^2 L^2} \left( \frac{5z^8}{32z_0^8} + \frac{z^{10}}{60z_0^{10}} + \frac{z^9}{12z_0^9} + \frac{11z^7}{84z_0^7} + \frac{z^6}{24z_0^6} \right), \quad (\text{A.6})$$

$$\phi(z) = 3\sqrt{2} \sinh^{-1} \left( \sqrt{\frac{z}{z_0}} \right),$$

$$A_t(z) = \mu + \rho \left( \frac{z_0 z^2}{2} + \frac{z^3}{3} \right). \quad (\text{A.7})$$

where  $z_0$ ,  $\mu$ , and  $\rho$  are integration constants and  $V_{21}$  is a constant from the dilaton potential and  $g_g$  is gauge coupling. The dilaton potential is given as

$$V_E(\phi) = -\frac{12}{L^2} - \frac{42 \sinh^4\left(\frac{\phi}{3\sqrt{2}}\right)}{L^2} - \frac{42 \sinh^2\left(\frac{\phi}{3\sqrt{2}}\right)}{L^2} - \frac{3V_{21} \sinh^{14}\left(\frac{\phi}{3\sqrt{2}}\right)}{35L^2} - \frac{3V_{21} \sinh^{12}\left(\frac{\phi}{3\sqrt{2}}\right)}{10L^2} - \frac{3V_{21} \sinh^{10}\left(\frac{\phi}{3\sqrt{2}}\right)}{10L^2} + \frac{\rho^2 z_0^8}{g_g^2 L^2} \left\{ \frac{\sinh^{24}\left(\frac{\phi}{3\sqrt{2}}\right)}{20L^2} + \frac{3 \sinh^{22}\left(\frac{\phi}{3\sqrt{2}}\right)}{10L^2} + \frac{59 \sinh^{20}\left(\frac{\phi}{3\sqrt{2}}\right)}{80L^2} + \frac{15 \sinh^{18}\left(\frac{\phi}{3\sqrt{2}}\right)}{16L^2} + \frac{5 \sinh^{16}\left(\frac{\phi}{3\sqrt{2}}\right)}{8L^2} + \frac{5 \sinh^{14}\left(\frac{\phi}{3\sqrt{2}}\right)}{28L^2} \right\}. \quad (\text{A.8})$$

This solution is also a generalized one given in [33].

In this paper, we have not discussed thermodynamical properties of these two sets of black hole solutions and possible applications in hQCD model from gauge/gravity duality.

## References

- [1] J. M. Maldacena, “The large N limit of superconformal field theories and supergravity,” *Adv. Theor. Math. Phys.* **2**, 231 (1998) [*Int. J. Theor. Phys.* **38**, 1113 (1999)] [arXiv:hep-th/9711200].
- [2] S. S. Gubser, I. R. Klebanov and A. M. Polyakov, “Gauge theory correlators from non-critical string theory,” *Phys. Lett. B* **428**, 105 (1998) [arXiv:hep-th/9802109].
- [3] E. Witten, “Anti-de Sitter space and holography,” *Adv. Theor. Math. Phys.* **2**, 253 (1998) [arXiv:hep-th/9802150].
- [4] O. Aharony, S. S. Gubser, J. M. Maldacena, H. Ooguri and Y. Oz, “Large N field theories, string theory and gravity,” *Phys. Rept.* **323**, 183 (2000) [arXiv:hep-th/9905111].
- [5] J. Erlich, E. Katz, D. T. Son, M. A. Stephanov, “QCD and a holographic model of hadrons,” *Phys. Rev. Lett.* **95**, 261602 (2005). [hep-ph/0501128].
- [6] G. F. de Teramond and S. J. Brodsky, “The hadronic spectrum of a holographic dual of QCD,” *Phys. Rev. Lett.* **94**, 201601 (2005).

- [7] L. Da Rold and A. Pomarol, “Chiral symmetry breaking from five dimensional spaces,” Nucl. Phys. B **721**, 79 (2005).
- [8] J. Babington, J. Erdmenger, N. J. Evans, Z. Guralnik and I. Kirsch, “Chiral symmetry breaking and pions in non-supersymmetric gauge/gravity Phys. Rev. D **69**, 066007 (2004) [arXiv:hep-th/0306018].
- [9] M. Kruczenski, D. Mateos, R. C. Myers and D. J. Winters, JHEP 0405 (2004) 041.
- [10] T. Sakai and S. Sugimoto, “Low energy hadron physics in holographic QCD,” Prog. Theor. Phys. **113**, 843 (2005); [arXiv:hep-th/0412141]. T. Sakai and S. Sugimoto, “More on a holographic dual of QCD,” Prog. Theor. Phys. **114**, 1083 (2006). [arXiv:hep-th/0507073].
- [11] C. Csaki and M. Reece, “Toward a systematic holographic QCD: A braneless approach,” JHEP **0705**, 062 (2007) [arXiv:hep-ph/0608266].
- [12] S. He, M. Huang, Q. S. Yan and Y. Yang, “Confront Holographic QCD with Regge Trajectories,” Eur.Phys.J.C.(2010)66:187. arXiv:0710.0988 [hep-ph].
- [13] E. V. Shuryak, Nucl. Phys. A **750**, 64 (2005) [arXiv:hep-ph/0405066]; M. J. Tannenbaum, Rept. Prog. Phys. **69**, 2005 (2006) [arXiv:nucl-ex/0603003].
- [14] G. Policastro, D. T. Son and A. O. Starinets, Phys. Rev. Lett. **87**, 081601 (2001) [arXiv:hep-th/0104066].
- [15] R. -G. Cai, Z. -Y. Nie, N. Ohta and Y. -W. Sun, “Shear Viscosity from Gauss-Bonnet Gravity with a Dilaton Coupling,” Phys. Rev. D **79**, 066004 (2009) [arXiv:0901.1421 [hep-th]].
- [16] R. -G. Cai, Z. -Y. Nie and Y. -W. Sun, “Shear Viscosity from Effective Couplings of Gravitons,” Phys. Rev. D **78**, 126007 (2008) [arXiv:0811.1665 [hep-th]].
- [17] S. J. Sin and I. Zahed, “Holography of radiation and jet quenching,” Phys. Lett. B **608**, 265 (2005) [arXiv:hep-th/0407215]; E. Shuryak, S. J. Sin and I. Zahed, “A Gravity Dual of RHIC Collisions,” J. Korean Phys. Soc. **50**, 384 (2007) [arXiv:hep-th/0511199].
- [18] H. Nastase, “The RHIC fireball as a dual black hole,” arXiv:hep-th/0501068.
- [19] R. A. Janik and R. B. Peshanski, “Asymptotic perfect fluid dynamics as a consequence of AdS/CFT,” Phys. Rev. D **73**, 045013 (2006) [arXiv:hep-th/0512162]; S. Nakamura and S. J. Sin, “A holographic dual of hydrodynamics,” JHEP **0609**, 020 (2006) [arXiv:hep-th/0607123]; S. J. Sin, S. Nakamura and S. P. Kim, “Elliptic Flow, Kasner Universe and Holographic Dual of RHIC Fireball,” JHEP **0612**, 075 (2006) [arXiv:hep-th/0610113].
- [20] C. P. Herzog, A. Karch, P. Kovtun, C. Kozcaz and L. G. Yaffe, “Energy loss of a heavy quark moving through  $N = 4$  supersymmetric Yang-Mills plasma,” JHEP **0607**, 013 (2006) [arXiv:hep-th/0605158]; S. S. Gubser, “Drag force in AdS/CFT,” Phys. Rev. D **74**, 126005 (2006) [arXiv:hep-th/0605182].
- [21] M. Rozali, H. -H. Shieh, M. Van Raamsdonk and J. Wu, “Cold Nuclear Matter In Holographic QCD,” JHEP **0801**, 053 (2008) [arXiv:0708.1322 [hep-th]].
- [22] O. DeWolfe, S. S. Gubser and C. Rosen, “A holographic critical point,” Phys. Rev. D **83**, 086005 (2011) [arXiv:1012.1864 [hep-th]].
- [23] N. Horigome and Y. Tanii, “Holographic chiral phase transition with chemical potential,” JHEP **0701**, 072 (2007) [arXiv:hep-th/0608198].

- [24] O. Bergman, G. Lifschytz and M. Lippert, “Holographic Nuclear Physics,” JHEP **0711**, 056 (2007) [arXiv:0708.0326 [hep-th]].
- [25] J. B. Kogut, M. A. Stephanov, “The phases of quantum chromodynamics: From confinement to extreme environments,” Camb. Monogr. Part. Phys. Nucl. Phys. Cosmol. **21**, 1-364 (2004).
- [26] M. A. Stephanov, “QCD phase diagram: An Overview,” PoS **LAT2006**, 024 (2006). [arXiv:hep-lat/0701002 [hep-lat]].
- [27] M. G. Alford, A. Schmitt, K. Rajagopal, T. Schafer, “Color superconductivity in dense quark matter,” Rev. Mod. Phys. **80**, 1455-1515 (2008). [arXiv:0709.4635 [hep-ph]].
- [28] U. Gursoy and E. Kiritsis, “Exploring improved holographic theories for QCD: Part I,” JHEP **0802**, 032 (2008) [arXiv:0707.1324 [hep-th]].
- [29] U. Gursoy, E. Kiritsis and F. Nitti, “Exploring improved holographic theories for QCD: Part II,” JHEP **0802**, 019 (2008) [arXiv:0707.1349 [hep-th]].
- [30] S. S. Gubser and A. Nellore, “Mimicking the QCD equation of state with a dual black hole,” Phys. Rev. D **78**, 086007 (2008); S. S. Gubser, A. Nellore, S. S. Pufu and F. D. Rocha, “Thermodynamics and bulk viscosity of approximate black hole duals to finite temperature quantum chromodynamics,” Phys. Rev. Lett. **101**, 131601 (2008); S. S. Gubser, S. S. Pufu and F. D. Rocha, “Bulk viscosity of strongly coupled plasmas with holographic duals,” JHEP **0808**, 085 (2008).
- [31] U. Gursoy, E. Kiritsis, L. Mazzanti and F. Nitti, “Deconfinement and Gluon Plasma Dynamics in Improved Holographic QCD,” Phys. Rev. Lett. **101**, 181601 (2008); U. Gursoy, E. Kiritsis, G. Michalogiorgakis and F. Nitti, “Thermal Transport and Drag Force in Improved Holographic QCD,” JHEP **0912**, 056 (2009).
- [32] E. Megias, H. J. Pirner and K. Veschgini, “QCD-Thermodynamics using 5-dim Gravity,” Phys. Rev. D **83**, 056003 (2011) [arXiv:1009.2953 [hep-ph]]; K. Veschgini, E. Megias and H. J. Pirner, “Trouble Finding the Optimal AdS/QCD,” Phys. Lett. B **696**, 495 (2011) [arXiv:1009.4639 [hep-th]]; E. Megias, H. J. Pirner and K. Veschgini, “Thermodynamics of AdS/QCD within the 5D dilaton-gravity model,” Nucl. Phys. Proc. Suppl. **207-208**, 333 (2010) [arXiv:1008.4505 [hep-th]]; B. Galow, E. Megias, J. Nian and H. J. Pirner, “Phenomenology of AdS/QCD and Its Gravity Dual,” Nucl. Phys. B **834**, 330 (2010) [arXiv:0911.0627 [hep-ph]].
- [33] D. Li, S. He, M. Huang and Q. S. Yan, “Thermodynamics of deformed AdS<sub>5</sub> model with a positive/negative quadratic correction in graviton-dilaton system,” arXiv:1103.5389 [hep-th].
- [34] S. He, Y. -P. Hu, J. -H. Zhang, “Hydrodynamics of a 5D Einstein-dilaton black hole solution and the corresponding BPS state,” [arXiv:1111.1374 [hep-th]].
- [35] C. Charmousis, B. Gouteraux, B. S. Kim, E. Kiritsis and R. Meyer, “Effective Holographic Theories for low-temperature condensed matter systems,” JHEP **1011**, 151 (2010) [arXiv:1005.4690 [hep-th]].
- [36] B. Gouteraux and E. Kiritsis, “Generalized Holographic Quantum Criticality at Finite Density,” JHEP **1112**, 036 (2011) [arXiv:1107.2116 [hep-th]].
- [37] O. DeWolfe, S. S. Gubser, C. Rosen, “Dynamic critical phenomena at a holographic critical point,” [arXiv:1108.2029 [hep-th]].
- [38] N. Evans, A. Gebauer, K. -Y. Kim, “E, B,  $\mu$ , T Phase Structure of the  $D3/D7$  Holographic Dual,” JHEP **1105**, 067 (2011). [arXiv:1103.5627 [hep-th]].



- [39] N. Evans, K. -Y. Kim, J. P. Shock, J. P. Shock, “Chiral phase transitions and quantum critical points of the  $D3/D7(D5)$  system with mutually perpendicular E and B fields at finite temperature and density,” *JHEP* **1109**, 021 (2011). [arXiv:1107.5053 [hep-th]].
- [40] N. Evans, A. Gebauer, K. -Y. Kim, “Towards a Holographic Model of the QCD Phase Diagram,” [arXiv:1109.2633 [hep-th]].
- [41] O. Andreev, “Cold Quark Matter, Quadratic Corrections and Gauge/String Duality,” *Phys. Rev. D* **81**, 087901 (2010) [arXiv:1001.4414 [hep-ph]].
- [42] E. Witten, “Anti-de Sitter space, thermal phase transition, and confinement in gauge theories,” *Adv. Theor. Math. Phys.* **2**, 505 (1998) [arXiv:hep-th/9803131].
- [43] C. P. Herzog, “A Holographic Prediction of the Deconfinement Temperature,” *Phys. Rev. Lett.* **98**, 091601 (2007) [hep-th/0608151].
- [44] R. -G. Cai and J. P. Shock, “Holographic confinement/deconfinement phase transitions of AdS/QCD in curved spaces,” *JHEP* **0708**, 095 (2007) [arXiv:0705.3388 [hep-th]].
- [45] B. H. Lee, C. Park and S. J. Sin, “A Dual Geometry of the Hadron in Dense Matter,” *JHEP* **0907**, 087 (2009) [arXiv:0905.2800 [hep-th]].
- [46] G. Mandal and T. Morita, “Gregory-Laflamme as the confinement/deconfinement transition in holographic QCD,” *JHEP* **1109**, 073 (2011) [arXiv:1107.4048 [hep-th]].
- [47] G. Mandal and T. Morita, “What is the gravity dual of the confinement/deconfinement transition in holographic QCD?,” arXiv:1111.5190 [hep-th].
- [48] O. Andreev and V. I. Zakharov, “The Spatial String Tension, Thermal Phase Transition, and AdS/QCD,” *Phys. Lett. B* **645**, 437 (2007) [arXiv:hep-ph/0607026].
- [49] O. Andreev and V. I. Zakharov, “On Heavy-Quark Free Energies, Entropies, Polyakov Loop, and AdS/QCD,” *JHEP* **0704**, 100 (2007) [arXiv:hep-ph/0611304];
- [50] O. Andreev, “Renormalized Polyakov Loop in the Deconfined Phase of  $SU(N)$  Gauge Theory and Gauge/String Duality,” *Phys. Rev. Lett.* **102**, 212001 (2009) [arXiv:0903.4375 [hep-ph]].
- [51] J. Noronha, “Connecting Polyakov Loops to the Thermodynamics of  $SU(N_c)$  Gauge Theories Using the Gauge-String Duality,” *Phys. Rev. D* **81**, 045011 (2010) [arXiv:0910.1261 [hep-th]].
- [52] D. f. Zeng, “Heavy quark potentials in some renormalization group revised AdS/QCD models,” *Phys. Rev. D* **78**, 126006 (2008) [arXiv:0805.2733 [hep-th]].
- [53] A. Karch, E. Katz, D. T. Son and M. A. Stephanov, “Linear Confinement and AdS/QCD,” *Phys. Rev. D* **74**, 015005 (2006) [arXiv:hep-ph/0602229].
- [54] J. Polchinski, M. J. Strassler, “Deep inelastic scattering and gauge / string duality,” *JHEP* **0305**, 012 (2003). [hep-th/0209211].
- [55] O. Andreev and V. I. Zakharov, “Heavy-quark potentials and AdS/QCD,” *Phys. Rev. D* **74**, 025023 (2006) [arXiv:hep-ph/0604204].
- [56] H. J. Pirner and B. Galow, “Strong Equivalence of the AdS-Metric and the QCD Running Coupling,” *Phys. Lett. B* **679**, 51 (2009) [arXiv:0903.2701 [hep-ph]].
- [57] S. He, M. Huang and Q. S. Yan, “Logarithmic correction in the deformed  $AdS_5$  model to produce the heavy quark potential and QCD beta function,” arXiv:1004.1880 [hep-ph].
- [58] F. Zuo, “Improved Soft-Wall model with a negative dilaton,” *Phys. Rev. D* **82**, 086011 (2010). arXiv:0909.4240 [hep-ph].

- [59] G. F. de Teramond and S. J. Brodsky, “Light-Front Holography and Gauge/Gravity Duality: The Light Meson and Baryon Spectra,” arXiv:0909.3900 [hep-ph].
- [60] A. Karch, E. Katz, D. T. Son and M. A. Stephanov, “On the sign of the dilaton in the soft wall models,” arXiv:1012.4813 [hep-ph].
- [61] R. Casero, E. Kiritsis and A. Paredes, “Chiral symmetry breaking as open string tachyon condensation,” Nucl. Phys. B **787**, 98 (2007) [hep-th/0702155 [HEP-TH]].
- [62] I. Iatrakis, E. Kiritsis and A. Paredes, “An AdS/QCD model from Sen’s tachyon action,” Phys. Rev. D **81**, 115004 (2010) [arXiv:1003.2377 [hep-ph]].
- [63] I. Iatrakis, E. Kiritsis and A. Paredes, “An AdS/QCD model from tachyon condensation: II,” JHEP **1011**, 123 (2010) [arXiv:1010.1364 [hep-ph]].
- [64] Y. -Q. Sui, Y. -L. Wu, Z. -F. Xie and Y. -B. Yang, “Prediction for the Mass Spectra of Resonance Mesons in the Soft-Wall AdS/QCD with a Modified 5D Metric,” Phys. Rev. D **81**, 014024 (2010) [arXiv:0909.3887 [hep-ph]].
- [65] Y. -Q. Sui, Y. -L. Wu and Y. -B. Yang, “Predictive AdS/QCD Model for Mass Spectra of Mesons with Three Flavors,” Phys. Rev. D **83**, 065030 (2011) [arXiv:1012.3518 [hep-ph]].
- [66] P. Zhang, “Linear Confinement for Mesons and Nucleons in AdS/QCD,” JHEP **1005**, 039 (2010) [arXiv:1003.0558 [hep-ph]].
- [67] P. Colangelo, F. Giannuzzi and S. Nicotri, “Holography, Heavy-Quark Free Energy, and the QCD Phase Diagram,” Phys. Rev. D **83**, 035015 (2011) [arXiv:1008.3116 [hep-ph]].
- [68] J. D. Bekenstein, Phys. Rev. D **7**, 2333 (1973); S. W. Hawking, Commun. Math. Phys. **43**, 199 (1975) [Erratum-ibid. **46**, 206 (1976)].
- [69] F. V. Gubarev, L. Stodolsky and V. I. Zakharov, “On the significance of the quantity  $A^{**2}$ ,” Phys. Rev. Lett. **86**, 2220 (2001) [arXiv:hep-ph/0010057]; F. V. Gubarev and V. I. Zakharov, “On the emerging phenomenology of  $\langle(A(a)(\mu))^{**2}(\min)\rangle$ ,” Phys. Lett. B **501**, 28 (2001) [arXiv:hep-ph/0010096].
- [70] J. M. Maldacena, “Wilson loops in large N field theories,” Phys. Rev. Lett. **80**, 4859 (1998) [arXiv:hep-th/9803002].
- [71] S. J. Rey, S. Theisen and J. T. Yee, “Wilson-Polyakov loop at finite temperature in large N gauge theory and anti-de Sitter supergravity,” Nucl. Phys. B **527**, 171 (1998) [arXiv:hep-th/9803135].
- [72] A. M. Polyakov, “String theory and quark confinement,” Nucl. Phys. Proc. Suppl. **68**, 1 (1998) [arXiv:hep-th/9711002].
- [73] J. Casalderrey-Solana, H. Liu, D. Mateos, K. Rajagopal and U. A. Wiedemann, “Gauge/String Duality, Hot QCD and Heavy Ion Collisions,” arXiv:1101.0618 [hep-th].
- [74] O. Andreev and V. I. Zakharov, “On Heavy-Quark Free Energies, Entropies, Polyakov Loop, and AdS/QCD,” JHEP **0704**, 100 (2007) [hep-ph/0611304].
- [75] U. Gursoy, E. Kiritsis, L. Mazzanti and F. Nitti, “Holography and Thermodynamics of 5D Dilaton-gravity,” JHEP **0905**, 033 (2009) [arXiv:0812.0792 [hep-th]].
- [76] M. Fromm, J. Langelage, S. Lottini and O. Philipsen, “The QCD deconfinement transition for heavy quarks and all baryon chemical potentials,” arXiv:1111.4953 [hep-lat].
- [77] Z. Fodor and S. D. Katz, “The Phase diagram of quantum chromodynamics,” arXiv:0908.3341 [hep-ph].

- [78] M. Buballa, “NJL model analysis of quark matter at large density,” *Phys. Rept.* **407**, 205 (2005) [hep-ph/0402234].
- [79] B. -J. Schaefer and J. Wambach, “The Phase diagram of the quark meson model,” *Nucl. Phys. A* **757**, 479 (2005) [nucl-th/0403039].
- [80] H. -Y. Chen, K. Hashimoto and S. Matsuura, “Towards a Holographic Model of Color-Flavor Locking Phase,” *JHEP* **1002**, 104 (2010) [arXiv:0909.1296 [hep-th]].
- [81] P. Basu, F. Nogueira, M. Rozali, J. B. Stang and M. Van Raamsdonk, “Towards A Holographic Model of Color Superconductivity,” *New J. Phys.* **13**, 055001 (2011) [arXiv:1101.4042 [hep-th]].
- [82] I. Shovkovy and M. Huang, “Gapless two flavor color superconductor,” *Phys. Lett. B* **564**, 205 (2003) [hep-ph/0302142].